Supporting Information

Enhancing ferromagnetic coupling in CrXY (X = O, S, Se; Y = Cl, Br, I) monolayers by turning the covalent character of Cr-X bonds

Hao-Ran Zhu[1],[†] Bin Shao[1,2],[*,†] and Xu Zuo[1,3,4*,†]

[1] *College of Electronic Information and Optical Engineering, Nankai University, Tianjin-300350, P.R. China,*

[2]*Tianjin Key Laboratory of Optoelectronic Sensor and Sensing Network Technology, Nankai University, Tianjin-300071, P.R. China,*

[3]*Key Laboratory of Photoelectronic Thin Film Devices and Technology of Tianjin, Nankai University, Tianjin-300071, P.R. China, and*

[4]*Engineering Research Center of Thin Film Optoelectronics Technology, Ministry of Education, Nankai University, Tianjin-300071, P.R. China*

E-mail: bshao@nankai.edu.cn; xzuo@nankai.edu.cn

[*]To whom correspondence should be addressed

[†1] College of Electronic Information and Optical Engineering, Nankai University, Tianjin-300350, P.R. China

[‡]

[2]Tianjin Key Laboratory of Optoelectronic Sensor and Sensing Network Technology, Nankai University, Tianjin-300071, P.R. China

[¶]

[3]Key Laboratory of Photoelectronic Thin Film Devices and Technology of Tianjin, Nankai University, Tianjin-300071, P.R. China

[§]

Section I. Additional results on CrXY monolayers

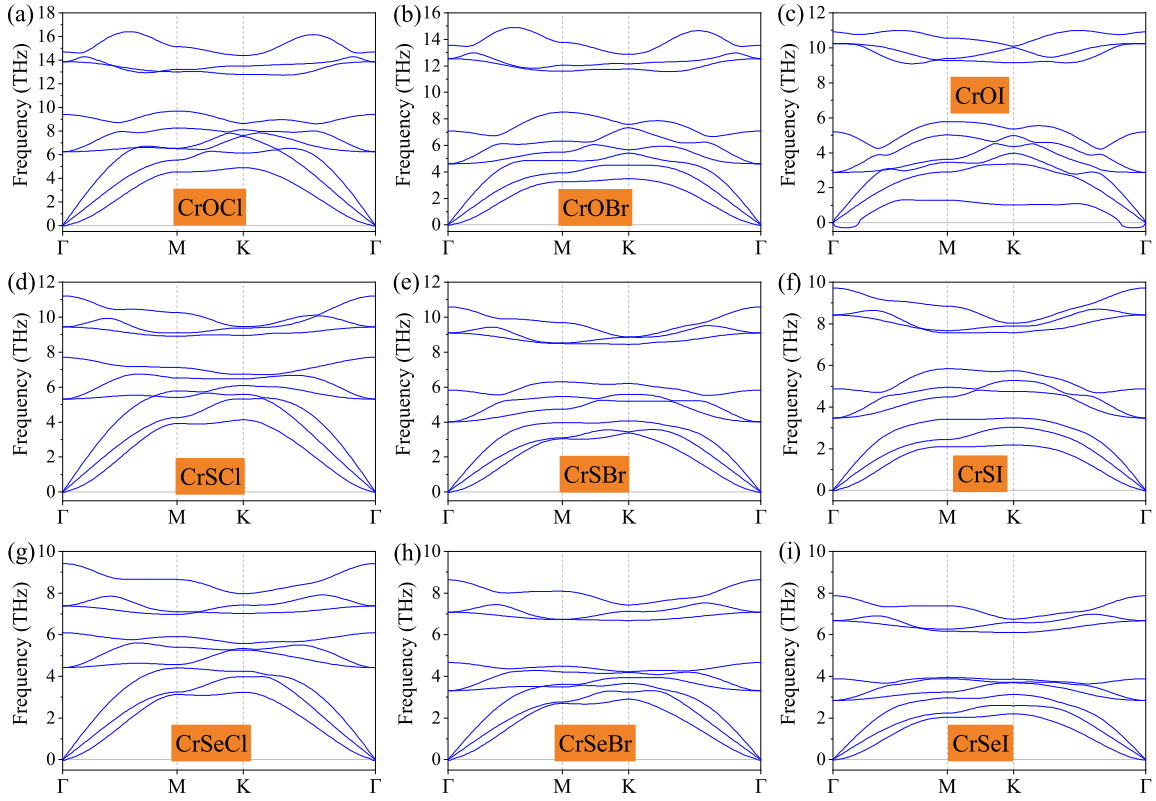

Fig. S1: Calculated phonon dispersions for the (a) CrOCl, (b) CrOBr, (c) CrOI, (d) CrSCl, (e) CrSBr, (f) CrSI, (g) CrSeCl, (h) CrSeBr and (i) CrSeI monolayers.

Table S1: Elastic constants of CrXY monolayers.

System	CrOCl	CrOBr	CrSCl	CrSBr	CrSI	CrSeCl	CrSeBr	CrSeI
C_{11}	451.289	564.104	272.730	262.598	257.217	231.091	223.921	216.463
C_{22}	449.828	564.041	273.587	263.765	256.883	231.280	223.481	216.341
C_{12}	105.175	154.032	59.479	56.925	53.149	52.796	50.821	46.101
C_{44}	171.509	136.443	107.097	103.252	102.162	89.268	86.473	85.261

[4]Engineering Research Center of Thin Film Optoelectronics Technology, Ministry of Education, Nankai University, Tianjin-300071, P.R. China

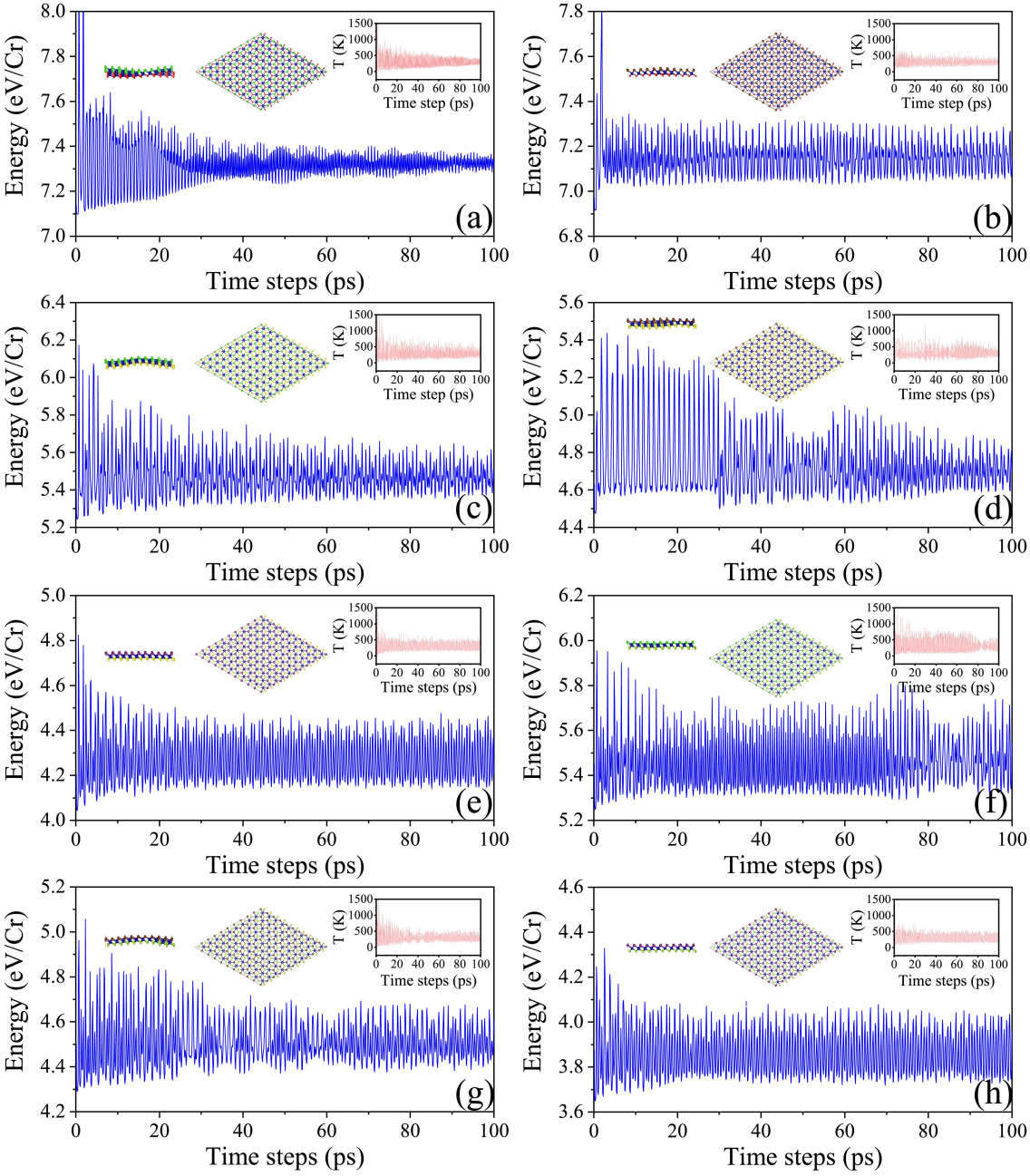

Fig. S2: Variations of total energy and temperature of against the time for the molecular dynamics simulation of (a) CrOCl, (b) CrOBr, (c) CrSCl, (d) CrSBr, (e) CrSI, (f) CrSeCl, (g) CrSeBr and (h) CrSeI monolayers are carried out with a universal force field as implemented in Forcite code, insert are top and side views of the snapshot of atomic configuration. The simulation is run under 300 K for 100 ps with a time step of 2 fs.

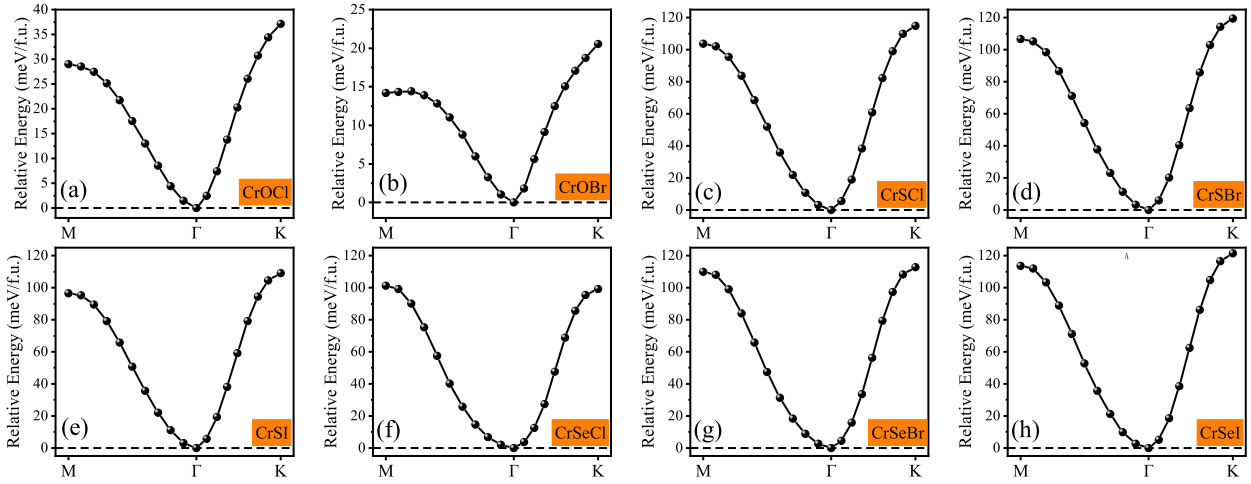

Fig. S3: Energy dependence on the magnetic propagation vector $\boldsymbol{q}$ of the (a) CrOCl, (b) CrOBr, (c) CrSCl, (d) CrSBr, (e) CrSI, (f) CrSeCl, (g) CrSeBr and (h) CrSeI monolayers.

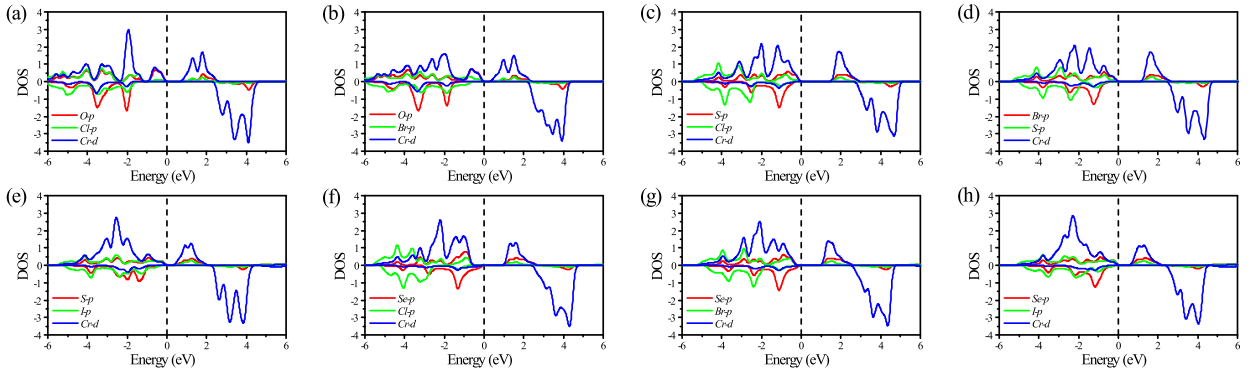

Fig. S4: Density of state (DOS) of the (a) CrOCl, (b) CrOBr, (c) CrSCl, (d) CrSBr, (e) CrSI, (f) CrSeCl, (g) CrSeBr and (h) CrSeI monolayers. The valence band maximum (VBM) energy is set to zero.

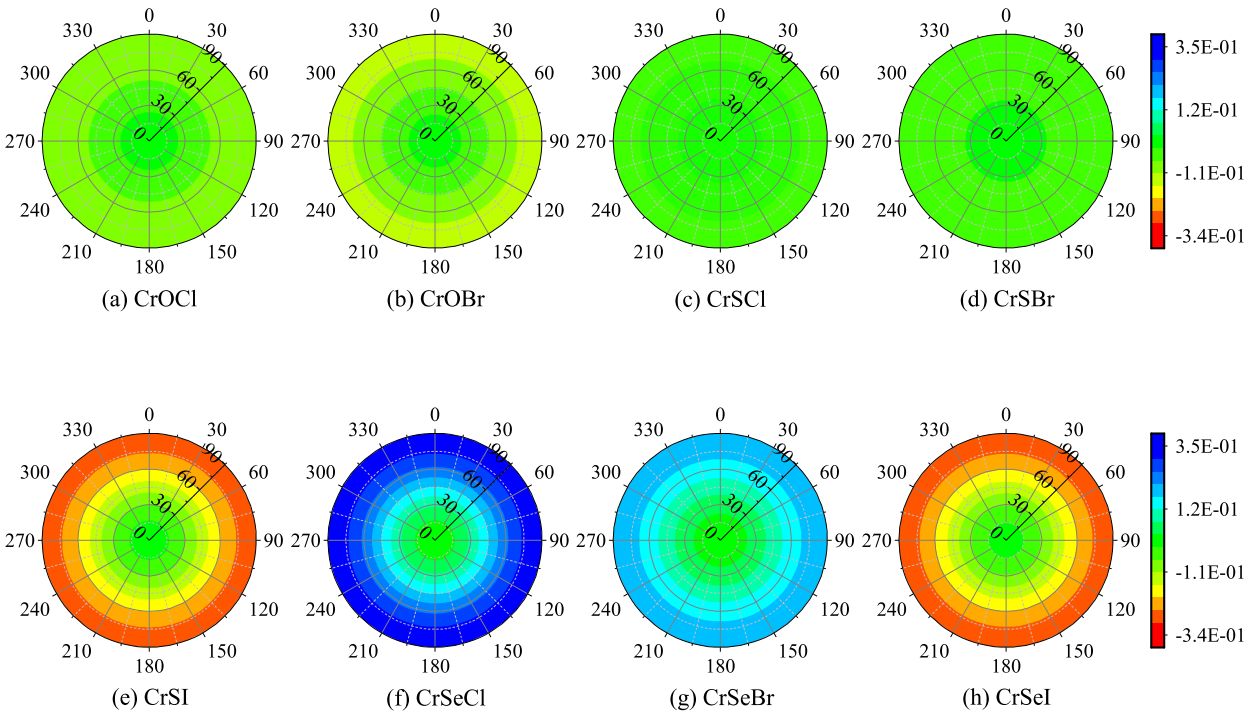

Fig. S5: Energies differences between the spin along different directions for (a) CrOCl, (b) CrOBr, (c) CrSCl, (d) CrSBr, (e) CrSI, (f) CrSeCl, (g) CrSeBr and (h) CrSeI monolayers, the energy of spin along the x-axis is chosen as the reference.

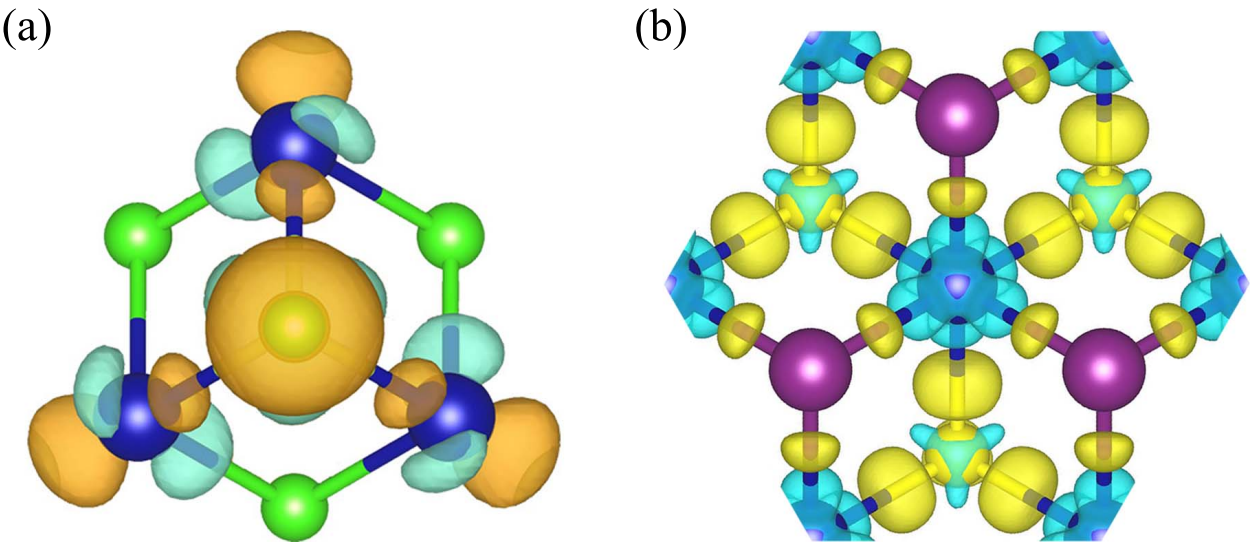

Fig. S6: (a) Hybridization of wave functions between the e_g- orbital of Cr atom and p_σ- orbital of S atom for CrSCl monolayer. (b) Differential charge density for CrSI, where yellow and cyan regions denote charge accumulation and depletion with the isosurface being set to 0.06 e/Å^3. The blue, yellow, green and purple balls represent the Cr atom, S atom, Cl atom and I atom, respectively.

Section II. The model of exchange mechanism

To understand exchange mechanism of CrXY monolayers, we consider a model from the perspective of the tight-binding theorem in which two transition-metal cations (two orbitals are involved, the lower orbital is half occupied and the higher one is empty) with an anion in-between, and the anion forms a 90° bridge between the two cations. The Hamiltonian for the model is given as (the second quantization is introduced as a simple notation of many-electron states)

$$\hat{H} = \hat{H}_M + \hat{H}_L + \hat{H}_t + \hat{H}_U \tag{1}$$

where the first two terms $\hat{H}_M$ and $\hat{H}_L$ are the on-site energy terms for the transition metal and anion ligand, respectively:

$$\hat{H}_M + \hat{H}_L = \sum_{i=l,r} \sum_{\mu=\alpha,\beta} \sum_{\sigma=\uparrow,\downarrow} \varepsilon_{i\mu} c^{\dagger}_{i\mu\sigma} c_{i\mu\sigma} + \sum_{\sigma=\uparrow,\downarrow} \varepsilon_p c^{\dagger}_{p\sigma} c_{p\sigma} \tag{2}$$

where l and r represent the two transition-metal sites, μ is the d-orbital index (μ = α, β), ε's are the on-site energies, $c^{\dagger}$ and c are the creation and annihilation operators, respectively. The third term $\hat{H}_t$ represents the hopping interaction between p- and d-orbitals:

$$\hat{H}_t = \sum_{i=l,r} \sum_{\mu=\alpha,\beta} \sum_{\sigma=\uparrow,\downarrow} t_{p\mu} (c^{\dagger}_{i\mu\sigma} c_{p\sigma} + c^{\dagger}_{p\sigma} c_{i\mu\sigma}) \tag{3}$$

The fourth term $\hat{H}_U$, describes the Coulomb repulsion between two electrons in d-orbital (the repulsion between electrons in the p-orbital is neglected):

$$\hat{H}_U = \sum_{i=l,r} \sum_{\mu=\alpha,\beta} U_{i\mu} n_{i\mu\uparrow} n_{i\mu\downarrow} \tag{4}$$

In the absence of hopping, the ground state will have two singly occupied d-orbitals (α, which is equivalent to t_{2g}) and two empty d-orbitals (β, which is equivalent to e_g), corresponding to a

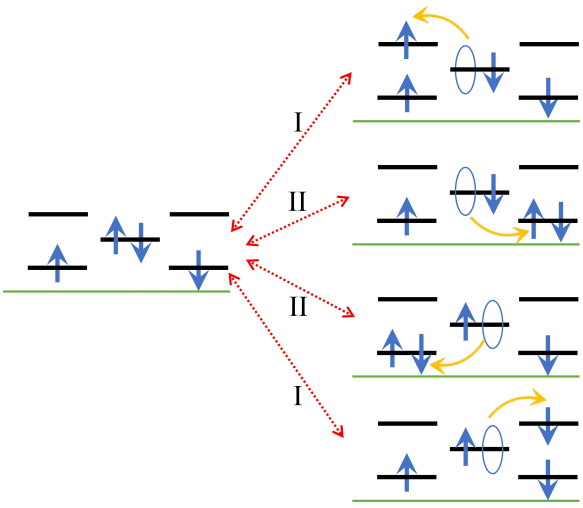

Fig. S7: Simple picture of superexchange for two d-spins point antiparallel, only one p-electron can hop to the cation on one side and come back, while the other p-electron with opposite spin must stay at the anion (i.e. the hopping process I or II, shown in Fig. 3).

positively charged transition-metal cation, and a doubly occupied p-orbital, corresponding to an anion ligand. First, we look at the case where the two d-spins point antiparallel (see Fig. S7). The Hamiltonian matrix in the corresponding Hilbert space is given by

$$\left(\begin{array}{c|cccc} 0 & t_1 & t_1 & t_2 & t_2 \\ \hline t_1 & \Delta_1 & 0 & 0 & 0 \\ t_1 & 0 & \Delta_1 & 0 & 0 \\ t_2 & 0 & 0 & U_d+\Delta_2 & 0 \\ t_2 & 0 & 0 & 0 & U_d+\Delta_2 \end{array}\right) \begin{array}{l} c^\dagger_{l-t_{2g}\uparrow}c^\dagger_{p\uparrow}c^\dagger_{p\downarrow}c^\dagger_{r-t_{2g}\uparrow}|0\rangle \\ c^\dagger_{l-t_{2g}\uparrow}c^\dagger_{l-e_g\uparrow}c^\dagger_{p\downarrow}c^\dagger_{r-t_{2g}\uparrow}|0\rangle \\ c^\dagger_{l-t_{2g}\uparrow}c^\dagger_{p\downarrow}c^\dagger_{r-e_g\uparrow}c^\dagger_{r-t_{2g}\uparrow}|0\rangle \\ c^\dagger_{l-t_{2g}\uparrow}c^\dagger_{l-t_{2g}\downarrow}c^\dagger_{p\uparrow}c^\dagger_{r-t_{2g}\uparrow}|0\rangle \\ c^\dagger_{l-t_{2g}\uparrow}c^\dagger_{p\uparrow}c^\dagger_{r-t_{2g}\downarrow}c^\dagger_{r-t_{2g}\uparrow}|0\rangle \end{array}$$

where $2\varepsilon_{t_{2g}\uparrow}+\varepsilon_{p\uparrow}+\varepsilon_{p\downarrow}$ has been chosen as the zero of energy, and we define $\Delta_1 = \varepsilon_{e_g\uparrow}$-$\varepsilon_{p\uparrow}$ and $\Delta_2 = \varepsilon_{t_{2g}\downarrow}$-$\varepsilon_{p\downarrow}$, t_1 and t_2 represent the hopping between p- and e_g-orbitals and p- and t_{2g}-orbitals, respectively. The basis states of the Hilbert space are given on the right and the lines indicate the partitioning of the Hilbert space for downfolding (The idea of downfolding is to partition the Hilbert space into parts that are of interest, here the low-energy covalent type states, and states that should be projected out, here the high-energy ionic states). The effective Hamiltonian for

antiparallel spins on d-orbitals is then

$$H_{\mathrm{AFM}} \approx (t_1,t_1,t_2,t_2) \begin{pmatrix} \varepsilon-\Delta_1 & 0 & 0 & 0 \\ 0 & \varepsilon-\Delta_1 & 0 & 0 \\ 0 & 0 & \varepsilon-U_d+\Delta_2 & 0 \\ 0 & 0 & 0 & \varepsilon-U_d+\Delta_2 \end{pmatrix}^{-1} \begin{pmatrix} t_1 \\ t_1 \\ t_2 \\ t_2 \end{pmatrix} \tag{5}$$
$$= -\frac{2t_1^2}{\Delta_1} - \frac{2t_2^2}{U_d+\Delta_2}$$

where in the last step we have set ε to zero.

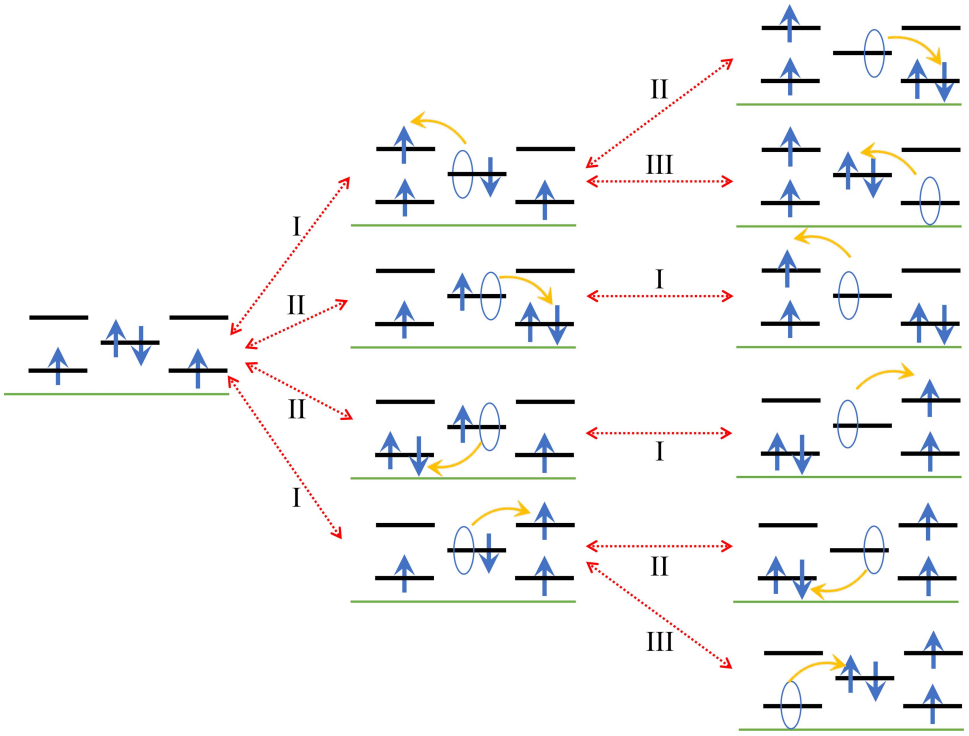

Fig. S8: Simple picture of superexchange for two d-spins point parallel, involves two fourth-order processes: two electrons from the p-orbital hopping to e_g- and t_{2g}-orbitals, and two coming back (i.e. the combination of hopping process I and II, shown in Fig. 3); one electron from the p-orbital hopping to e_g-orbital, then electron from the e_g-orbital hopping to p-orbital, and coming back (i.e. the combination of hopping process I and III, shown in Fig. 3).

For both d-spins point upwards, the dimensionality in the Hilbert space is nine. Starting from the ground state with two singly occupied t_{2g}-orbitals and two empty e_g-orbitals, the second group

has one of the p-electrons can transfer to a d-orbital, leading to one doubly occupied t_{2g} or one singly occupied e_g, while the last group has a second electron hop, leading to either an empty p- or t_{2g}-orbital. The corresponding Hamiltonian matrix is

$$\left(\begin{array}{c|cccc|cccc}
0 & t_1 & t_1 & t_2 & t_2 & 0 & 0 & 0 & 0 \\
\hline
t_1 & \Delta_1 & 0 & 0 & 0 & t_2 & 0 & t_2 & 0 \\
t_1 & 0 & \Delta_1 & 0 & 0 & 0 & t_2 & 0 & t_2 \\
t_2 & 0 & 0 & U_d+\Delta_2 & 0 & t_1 & 0 & 0 & 0 \\
t_2 & 0 & 0 & 0 & U_d+\Delta_2 & 0 & t_1 & 0 & 0 \\
\hline
0 & t_2 & 0 & t_1 & 0 & U_d+\Delta_1+\Delta_2 & 0 & 0 & 0 \\
0 & 0 & t_2 & 0 & t_1 & 0 & U_d+\Delta_1+\Delta_2 & 0 & 0 \\
0 & t_2 & 0 & 0 & 0 & 0 & 0 & \Delta_{\mathrm{CF}} & 0 \\
0 & 0 & t_2 & 0 & 0 & 0 & 0 & 0 & \Delta_{\mathrm{CF}}
\end{array}\right)
\begin{array}{l}
c^\dagger_{l-t_{2g}\uparrow}c^\dagger_{p\uparrow}c^\dagger_{p\downarrow}c^\dagger_{r-t_{2g}\uparrow}|0\rangle \\
c^\dagger_{l-t_{2g}\uparrow}c^\dagger_{l-e_g\uparrow}c^\dagger_{p\downarrow}c^\dagger_{r-t_{2g}\uparrow}|0\rangle \\
c^\dagger_{l-t_{2g}\uparrow}c^\dagger_{p\downarrow}c^\dagger_{r-e_g\uparrow}c^\dagger_{r-t_{2g}\uparrow}|0\rangle \\
c^\dagger_{l-t_{2g}\uparrow}c^\dagger_{l-t_{2g}\downarrow}c^\dagger_{p\uparrow}c^\dagger_{r-t_{2g}\uparrow}|0\rangle \\
c^\dagger_{l-t_{2g}\uparrow}c^\dagger_{p\uparrow}c^\dagger_{r-t_{2g}\downarrow}c^\dagger_{r-t_{2g}\uparrow}|0\rangle \\
c^\dagger_{l-t_{2g}\uparrow}c^\dagger_{l-e_g\uparrow}c^\dagger_{r-t_{2g}\downarrow}c^\dagger_{r-t_{2g}\uparrow}|0\rangle \\
c^\dagger_{l-t_{2g}\uparrow}c^\dagger_{l-t_{2g}\downarrow}c^\dagger_{r-e_g\uparrow}c^\dagger_{r-t_{2g}\uparrow}|0\rangle \\
c^\dagger_{l-t_{2g}\uparrow}c^\dagger_{l-e_g\uparrow}c^\dagger_{p\uparrow}c^\dagger_{p\downarrow}|0\rangle \\
c^\dagger_{p\uparrow}c^\dagger_{p\downarrow}c^\dagger_{r-e_g\uparrow}c^\dagger_{r-t_{2g}\uparrow}|0\rangle
\end{array}$$

where $\Delta_{\mathrm{CF}} = \varepsilon_{e_g}$-$\varepsilon_{t_{2g}}$. Downfolding the high energy states and setting $\varepsilon = 0$ (remembering $(A + \Delta)^{-1} \approx A^{-1}(1 - \Delta A^{-1})$), leads to

$$H_{\mathrm{FM}} \approx -\frac{2t_1^2}{\Delta_1} - \frac{2t_2^2}{U_d+\Delta_2} - 2(\frac{t_1t_2}{\Delta_1} + \frac{t_1t_2}{U_d+\Delta_2})^2\frac{1}{U_d+\Delta_1+\Delta_2} - 2(\frac{t_1t_2}{\Delta_1})^2\frac{1}{\Delta_{\mathrm{CF}}} \tag{6}$$

The first two terms are the same as for antiparallel spin (5).According to $\hat{H}_{12} = H_{\mathrm{FM}} - H_{\mathrm{AFM}} = -JS_1S_2$ and set $S_1 = S_2 = 3/2$, we have

$$J = -\frac{8}{9}(\frac{t_1t_2}{\Delta_1} + \frac{t_1t_2}{U_d+\Delta_2})^2\frac{1}{U_d+\Delta_1+\Delta_2} - \frac{8}{9}(\frac{t_1t_2}{\Delta_1})^2\frac{1}{\Delta_{\mathrm{CF}}} \tag{7}$$

There is still a direct exchange interaction between transition-metal cations, which is AFM. However, the direct AFM exchange of CrXY monolayers are weak because of the large distance (> 3.1 Å) between adjacent Cr ions, it can be ignored.

Table S2: Hopping interaction between p- and e_g-orbitals (t_1) and p- and t_{2g}-orbitals (t_2) of CrXY monolayers.

System	CrOCl	CrOBr	CrSCl	CrSBr	CrSI	CrSeCl	CrSeBr	CrSeI
t_1	-0.18	-0.08	-0.54	-0.46	-0.34	-0.59	-0.52	-0.42
t_2	-0.70	-0.66	-0.52	-0.52	-0.52	-0.43	-0.44	-0.46